ELSEVIER

Carbohydrate Research 300 (1997) 59–66

CARBOHYDRATE RESEARCH

Study of the phase space structure for a two-degrees of freedom model of a symmetric glycosidic linkage

Sergio Abbate [a,*], Luca Biancardi [a], Giovanna Longhi [a], Giuseppina Conti [b]

[a] *Dipartimento di Scienze Biomediche e Biotecnologie, Università di Brescia, via Valsabbina 19, 25123 Brescia, Italy*

[b] *Istituto di Ricerca "G. Donegani", via Fauser 4, 28100 Novara, Italy*

Received 8 October 1996; accepted 24 January 1997

Abstract

Classical dynamics calculations have been carried out on a two-degrees of freedom model Hamiltonian representing the symmetric glycosidic linkage of β,β-trehalose. The Hamiltonian depends on coordinates Φ and Φ' and their conjugate momenta, where Φ and Φ' are the torsional angles M–C-1–O-1–C-1′ and M′–C-1′–O-1–C-1 defined by the carbon and oxygen atoms of the glycosidic linkage and by pseudo-atoms M and M′ representing the effect of the pyranose rings. We have employed a simplified potential function reproducing the major features of molecular mechanics results in the literature. All relevant initial conditions for energy values ranging up to the energy of rotation have been tried. Results have been examined by considering the plots $\Phi(t)$ and $\Phi'(t)$, the trajectories in the configuration space (Φ,Φ') for single initial conditions, and the Poincaré Surfaces of Sections, which describe the behavior of the system in the phase space, for all initial conditions at fixed energy. © 1997 Elsevier Science Ltd.

Keywords: Glycosidic linkage; β,β-Trehalose; Molecular Dynamics; Poincaré Surfaces of Sections

1. Introduction

Molecular dynamics (MD) calculations have become relatively common in the last ten years for biomolecules [1]: they are used in the solution of Newton's equations of motion, as they were previously in other fields such as celestial mechanics [2] and small molecules' vibrational dynamics [3–5]. The routines for performing the dynamical calculations [1] have been implemented on well-established molecular mechanics programs, allowing the minimization of the free energy as well as the minimization of the energy function. In addition, such programs allow a direct look at the real molecular motions, besides calculating interesting dynamical

* Corresponding author. Tel.: +39-030-37151-3715255; fax: +39-030-3701157.

PII S0008-6215(97)00033-5

properties like auto-correlation or cross-correlation functions of relevant degrees of freedom [3–6].

Sugar molecules, in particular mono- and oligosaccharides, have been treated with MD [6–9] to gain insight into a number of fascinating problems, such as the anomeric effect, the influence of the exo-groups on the conformation of the pyranose ring, the mobility of the glycosidic linkage, and the competition of hydration by water molecules with the internal hydrogen bonding. Last but not least such molecules are systems of low-to-medium dimensionality. MD programs solve Newton's equations, taking into account all degrees of freedom and sampling initial conditions from the conformation of minimum energy with a random choice of velocities compatible with the equipartition principle at the chosen temperature. The results thus obtained give an idea of the mobility of the system in the proposed minimum free-energy conformation.

Our approach is different, since we wish to describe the full vibrational dynamics in phase space of the glycosidic linkage, for all possible energies and all starting positions. In order to do this we have simplified the problem of the dynamics of a disaccharide to a two-dimensional system. For Hamiltonians which are not too different from integrable ones, the KAM theorem establishes the dynamics [10]. Instead, for highly anharmonic systems one has to try a numerical approach, in order to arrive at even a qualitative picture. In the case of two-dimensional systems, a considerable help in interpreting and understanding the numerical results comes from the consideration of the Poincaré Surfaces of Section (PSS) [10], which will be described below and constitutes the main tool of investigation of the present work.

2. Experimental

In our model we deal with the torsional internal coordinates Φ and Φ' around the C-1–O-1 and C-1′–O-1 glycosidic bonds, respectively, of β,β-trehalose. Following Wilson et al. [11] the torsional coordinates are variations of dihedral angles of two 'molecular' planes having the C-1–O-1 (or C-1′–O-1) bond in common. At this point we define Φ as the instantaneous value of the dihedral angle formed by M–C-1–O-1 and C-1–O-1–C-1′ (M–C-1–O-1–C-1′) and Φ' as that of the dihedral angle formed by M′–C-1′–O-1 and C-1′–O-1–C-1 (M′–C-1′–O-1–C-1); M and M′ are pseudo-atoms that take into account the effect of the two respective pyranose rings (see Fig. 1, top). Their mass is the same as the whole mass of the pyranose ring (except for C-1 or C-1′); their position is on the C-1–C-4 (C-1′–C-4′) line at a distance from C-1 (C-1′) such that the moment of inertia of M (M′) about C-1–O-1 (C-1′–O-1) is the same as the moment of inertia of the whole pyranose ring about the same axis. The motivation for such a definition of M (M′) is the fact that the coefficients given by Decius [12] for the kinetic energy depend on the moments of inertia of the four atoms with respect to an axis that here we approximate to be the bond C-1–O-1 (C-1′–O-1). The pyranose ring conformation is assumed to be a perfect $^4C_1$ chair, and H, OH, and the CH_2OH groups are assumed to be 'condensed' onto the carbon atoms to which they are

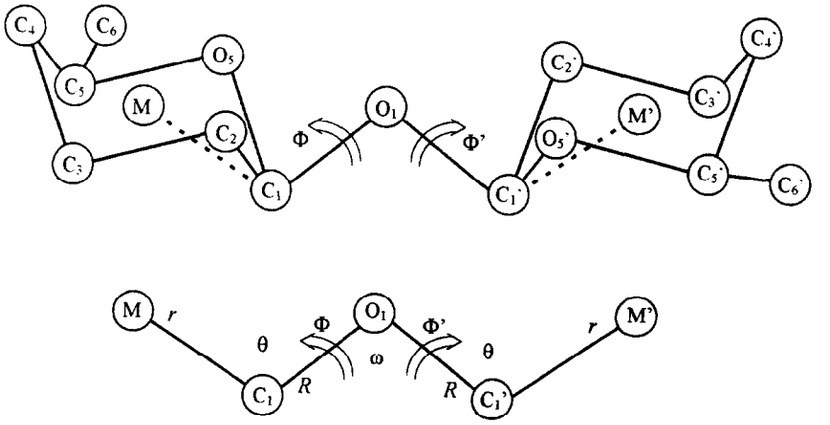

Fig. 1. Definition of the pseudo-masses M and M′ representing the effect of the pyranose rings in β,β-trehalose in Φ and Φ', and definition of the torsional coordinates Φ and Φ' (top); definition of the bond distances and interbond angles used in the calculation of the kinetic energy coefficients of eq. (2′) (bottom).

attached. Thus the value of the mass of M and M′ is 151 amu, the M–C-1 and M′–C-1′ distances are 2.95 Å, and the angles M–C-1–O-1 (M′–C-1′–O-1) are 150.5°. The Hamiltonian function is:

$$H = \tfrac{1}{2}g(\Phi)p_\Phi^2 + \tfrac{1}{2}g(\Phi')p_{\Phi'}^2 + g'(\Phi,\Phi')p_\Phi p_{\Phi'} + V(\Phi,\Phi') \quad (1)$$

where p_Φ and p'_Φ are the moments conjugated to Φ and Φ', respectively. According to Decius [12] $g(\Phi)$ and $g'(\Phi,\Phi')$ are:

$$\begin{aligned} g(\Phi) &= A_2 + (1/m_O)\left[(B_1 - C_2)^2 + C_1^2\right] \\ &\quad + (1/m_C)\left[(B_2 - C_1)^2 + C_2^2\right] \\ &\quad + 2\left[(C_2 - B_1)C_1/m_O \right. \\ &\quad \left. + (C_1 - B_2)C_2/m_C\right]\cos\Phi \end{aligned} \quad (2)$$

$$\begin{aligned} g'(\Phi,\Phi') &= 2A_1C_2 - (1/m_O)(B_1 - C_2)^2 \\ &\quad + \left[A_1(C_1 - B_2) + (1/m_O)C_1(B_1 - C_2)\right] \\ &\quad \times(\cos\Phi + \cos\Phi') - \left(C_1^2/m_O\right) \\ &\quad \times(\cos\Phi\cos\Phi' + \cos\omega\sin\Phi\sin\Phi') \end{aligned} \quad (2')$$

where

$$C_1 = \cot\theta/R$$

$$C_2 = \cot\omega/R$$

$$A_1 = \left(m_C R\sin\omega\right)^{-1}$$

$$A_2 = \left(m_C R^2\sin^2\omega\right)^{-1} + \left(m_M r^2\sin^2\theta\right)^{-1}$$

$$B_1 = \left(R\sin\omega\right)^{-1}$$

$$B_2 = \left(r\sin\theta\right)^{-1}$$

where m_C, m_O, and m_M are the masses of C, O, and M atoms, and the remaining symbols are defined in Fig. 1, bottom.

The potential function that we used in Eq. (1) is:

$$\begin{aligned} V(\Phi,\Phi') &= A[1 - \cos(\Phi + 120°)] + A[1 - \cos(\Phi' + 120°)] \\ &\quad + B[1 - \cos(\Phi + 120°)][1 - \cos(\Phi' + 120°)] \end{aligned} \quad (3)$$

with $A = 1050\ \text{cm}^{-1} = 12.5$ kJ/mole; $B = 210\ \text{cm}^{-1} = 2.5$ kJ/mole.

Eq. (3) provides the major features of the level curves calculated by Tvaroska and Vaklavik [13] for a model molecule of β,β'-trehalose, taking into account that they use a coordinate φ which is the tetrahedral angle O-5–C-1–O-1–C-1′ related to our $\Phi = \varphi - 60°$.

The potential (3) exhibits two orthogonal rotation paths with a barrier height of about $E_{esc} = 2100\ \text{cm}^{-1} = 25$ kJ/mole and introduces an absolute maximum for V at $5040\ \text{cm}^{-1} = 60$ kJ/mole; of course many other features predicted by the paper cited are missed by Eq. (3). Other level curves reported more recently in the literature for trehalose (see, e.g., Ref. [14]) have not jet been considered here.

The equations of motion resulting from Hamiltonian (1) are [15]:

$$\begin{aligned} (\mathrm{d}\Phi/\mathrm{d}t) &= \partial H/\partial p_\Phi = g(\Phi)p_\Phi + g'(\Phi,\Phi')p_{\Phi'} \\ (\mathrm{d}\Phi'/\mathrm{d}t) &= \partial H/\partial p_{\Phi'} = g(\Phi')p_{\Phi'} + g'(\Phi,\Phi')p_\Phi \\ (\mathrm{d}p_\Phi/\mathrm{d}t) &= -\partial H/\partial\Phi \\ &= -(\partial g/\partial\Phi)p_\Phi^2 - (\partial g'/\partial\Phi)p_\Phi p_{\Phi'} - (\partial V/\partial\Phi) \\ &= f_\Phi + F_\Phi \\ (\mathrm{d}p_{\Phi'}/\mathrm{d}t) &= -\partial H/\partial\Phi' \\ &= -(\partial g/\partial\Phi')p_{\Phi'}^2 - (\partial g'/\partial\Phi')p_\Phi p_{\Phi'} - (\partial V/\partial\Phi') \\ &= f_{\Phi'} + F_{\Phi'} \end{aligned} \quad (4)$$

The third and fourth equations in particular state that the derivatives with respect to time of the generalized momenta p_Φ and $p_{\Phi'}$ are the generalized forces; in this case the latter are the sums of F_Φ ($F_{\Phi'}$), which are minus the derivatives of the potential V with respect to the generalized coordinates, and of f_Φ ($f_{\Phi'}$), which are tensions originating from the constraints given by the Φ and Φ' dependence of the kinetic energy coefficients. Eqs. (4) have been numerically integrated into a home-made program that makes use of a fourth-order Runge–Kutta routine of the SSP library [16]; the integration step was 0.07 fs; total integration times varied up to 1 ns for irregular or higher-resonances orbits (see below). The results of the integration are the time evolutions $\Phi(t)$, $\Phi'(t)$, $p_\Phi(t)$, and $p_{\Phi'}(t)$. In order to get an idea of the dynamical properties of the system up to the energy of rotation, we ran calculations for groups with different initial conditions, each group having the same energy value; the energy is also an initial condition and is a constant. For each initial condition we produced three different kinds of plot:

(i) $\Phi(t)$ and $\Phi'(t)$ and their combinations $\Phi(t) + \Phi'(t)$ and $\Phi(t) - \Phi'(t)$;

(ii) the curves in the (Φ,Φ') plane defined by the points visited by the system during its time evolution; we will refer to these as Lissajous maps;

(iii) PSSs [10], which represent the behavior in the phase space of the second oscillator (Φ', $p_{\Phi'}$) when the first one goes through a fixed position $\Phi = \Phi^*$, which in our case has been chosen as the minimum of the potential V, namely $\Phi = \Phi^* = -120°$. This type of map, which has been widely used first in celestial mechanics [10], is a stroboscopic description of one of the oscillators as seen by the other. It allows us to define the full four-dimensional dynamical state through two-dimensional curves. Indeed, knowing the energy E, Φ^*, and the values of Φ' and $p_{\Phi'}$ in a given PSS curve, one can derive the fourth variable p_Φ by inverting Eq. (1), namely:

$$p_\Phi = \frac{-g'(\Phi^*,\Phi')}{g(\Phi^*)} p_{\Phi'} \pm \frac{\sqrt{g'(\Phi^*,\Phi')^2 - 2g(\Phi^*)[V(\Phi^*,\Phi') - E]}}{g(\Phi^*)} \quad (5)$$

Of course there is an ambiguity in the sign in Eq. (5). in order to solve it, we define the PSSs as the curves in the phase space for:

$$\Phi = \Phi^* = -120° \qquad p_\Phi > \frac{-g'(\Phi^*,\Phi')}{g(\Phi^*)} p_{\Phi'} \quad (6)$$

The construction of the PSSs with conditions (6) allows unambiguous definition of the dynamical state of the system through Eq. (5) with the + sign. Incidentally we notice that, had the kinetic energy coefficients been constant (as in the majority of the cases studied) the second equation in (6) would have been substituted by $p_\Phi > 0$ [10]. Finally, Eq. (5) was used as well to generate the initial conditions for obtaining PSS curves close to another PSS curve of the same energy E generated on the computer screen.

3. Results and discussion

In Fig. 2 we present the PSSs for six significant values of the energy E up to the threshold for rotation E_{esc}, which is 2100 cm^{-1}. Different colors correspond generally to different initial conditions; due to limited availability in the number of colors, occasionally two different trajectories may have been traced with the same color; however, we made sure that adjacent trajectories never have the same color.

For the lowest value of the energy, at about 5% of E_{esc}, we have the PSS set of curves at the top left corner: each initial condition generates a regular trajectory. There are two families of closed curves [1] around two centers, called fixed points [10]. The latter correspond to exactly **periodic modes**, namely to the symmetric normal mode in the top part (where both p_Φ and $p_{\Phi'}$ have the same sign), and to the antisymmetric normal mode at the bottom of the PSS (where p_Φ and $p_{\Phi'}$ have opposite sign). This has also been observed in similar calculations performed for different two-dimensional systems such as two coupled Morse oscillators [4,5,17] or the Hénon–Heiles [18,10] Hamiltonian. The closed curves surrounding the fixed points correspond to **multiperiodic modes** [10], in that the symmetric and antisymmetric character is not completely lost, but a dephasing from the exact 0° or 180° phase difference comes in and goes off regularly in time, i.e. they exhibit a second period which is the time to recover the initial phase difference. This fact has been checked by $\Phi(t)$ and $\Phi'(t)$ plots, as carried out in Ref. [17]. Finally it can be seen that, while the symmetric fixed point is exactly at $\Phi' = -120°$, the antisymmetric one is at a slightly higher absolute value for Φ'. This phenomenon is observed at all energies and is more pronounced at higher E values; it is related to the presence of constraint tensions f_Φ and $f_{\Phi'}$. As a consequence, when running MD calculations one cannot disregard initial conditions off the 'natural' equilibrium.

At the next value of the energy E, at 14% of E_{esc} (top right corner), a third family of regular curves is observed besides the symmetric and antisymmetric normal modes families; each curve in this new family is composed of four non-connected circles surrounding four fixed points; three of them are in the central part of the figure and one is squeezed into the bottom part on the right. Looking at the plots of $[\Phi(t) +$

[1] In Fig. 2 there are also regular trajectories that do not close. They indeed close 'outside' the figure, since the phase space available at fixed energy is not bounded by any trajectory in this coordinates system [10].

Fig. 2. Poincaré Surfaces of Section for six values of the energy E in the plane Φ' (phi' in the figures) and $p_{\Phi'}$ ($p_{phi'}$ in the figures). Units for Φ' are degrees and for $p_{\Phi'}$ are $u^* = amu\,Å^2\,°/fs$. Each color corresponds to a different initial condition (see text).

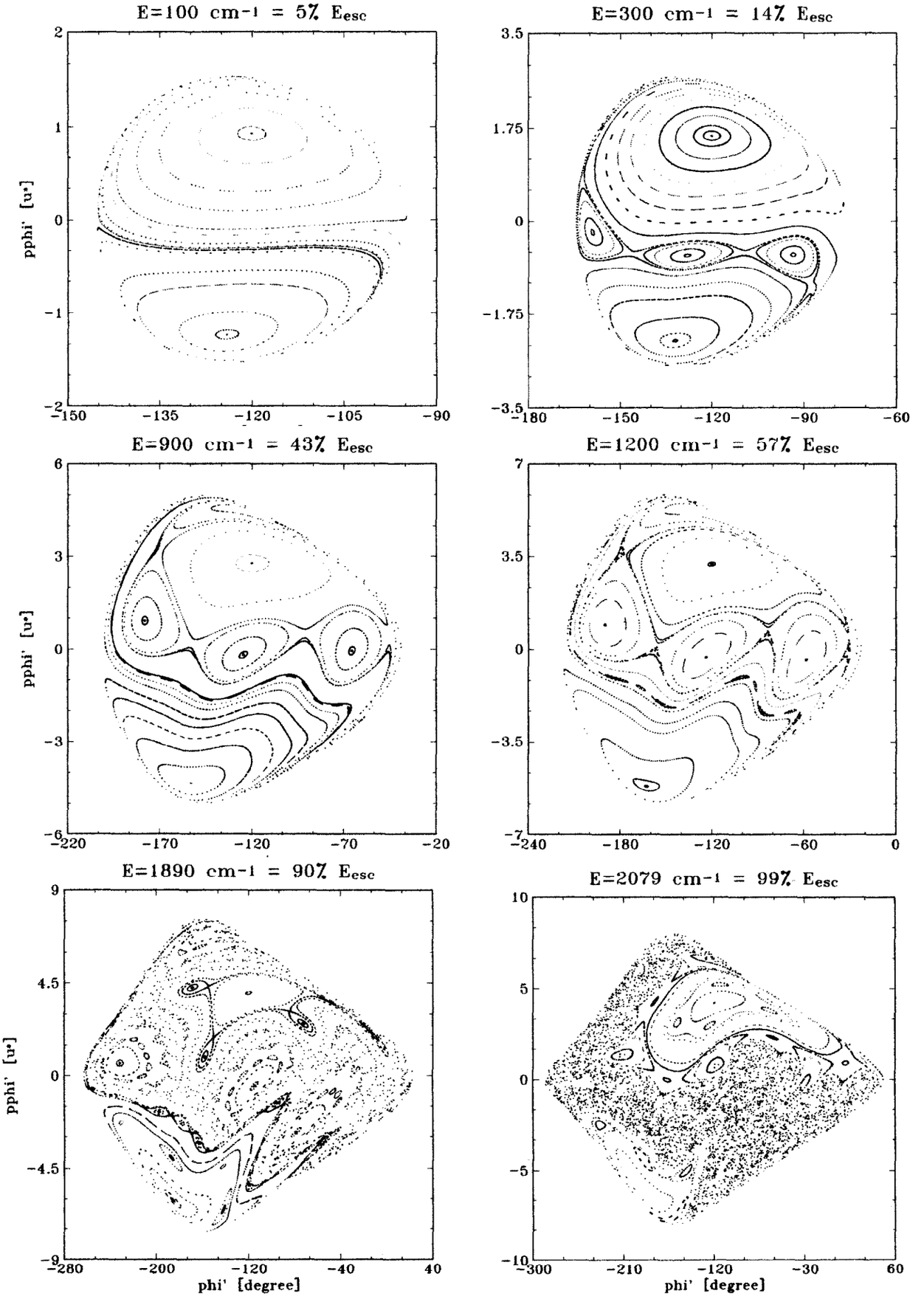
E=100 cm-1 = 5% Eesc
E=300 cm-1 = 14% Eesc
E=900 cm-1 = 43% Eesc
E=1200 cm-1 = 57% Eesc
E=1890 cm-1 = 90% Eesc
E=2079 cm-1 = 99% Eesc
pphi' [u']
phi' [degree]

$\Phi'(t)]$ and $[\Phi(t) - \Phi'(t)]$ for the multiple fixed point, one realizes that this is a **resonant mode** [10], where the period of the symmetric coordinate is exactly 3:4 of the period of the antisymmetric coordinate. We observe that the appearance of this new family of curves is similar to that in the Hénon–Heiles system [18,10]. This is different from what happens for two coupled Morse oscillators, where new families of curves appear when one of the two main fixed points becomes unstable, and not at the separatrix between the two normal modes families. In that case these new families are the local modes [4,5,17].

The region of these higher-order resonance curves grows with increasing energy, as can be seen from the middle sets of PSSs corresponding to about 43% and 57% of E_{esc}. In the latter case another set of higher resonant modes appears in a thin layer near the separatrix between antisymmetric modes and the 3:4 resonance. The new fixed points of still higher multiplicity correspond to a 7:10 ratio in the frequencies of the symmetric to the antisymmetric normal coordinates. These resonant modes can be better studied at higher energy, where they occupy a larger portion of the phase space (see Fig. 3).

Further insight into the meaning of the fixed points can be gained also from the consideration of their Lissajous maps; in Fig. 3 we report the PSSs at $E = 1500\ cm^{-1} = 71\%$ of E_{esc}, together with the Lissajous maps of the four kinds of fixed points; we note that the symmetric and antisymmetric fixed points are 1:1 resonances of the two torsions.

Finally in the bottom part of Fig. 2, the ensemble of PSS curves for $E = 90\%$ of E_{esc} and for $E = 99\%$ of E_{esc} is given. Close to the resonances of higher order, trajectories appear that do not have the aspect of lines but of dots irregularly spread around. They correspond to **chaotic modes** [10] and tend to occupy larger and larger portions of the phase space. At these energies for which chaos becomes important, many other higher resonances appear. Chaotic modes eventually lead to rotation when the energy is higher than E_{esc}. This can be appreciated by comparing the Lissajous maps of two chaotic trajectories, one well below rotation (Fig. 4, top), and the other just above it (Fig. 4, bottom). Furthermore, we observe that many regular trajectories persist close to the rotational energy E_{esc} (and even beyond it). In particular the antisymmetric and symmetric normal modes look very stable, even if they get surrounded by other resonances.

We can draw the conclusions below which are based on a preliminary model of β,β-trehalose and needs major improvements especially in the potential function $V(\Phi,\Phi')$. We hope though to give an idea on the potentialities of these classical methods, with respect to what can be obtained either from Molecular Mechanics or ab-initio calculations.

In summary, we have described the qualitative features of the oscillatory dynamics of the glycosidic linkage in β,β-trehalose. In particular from zero energy up to about 10% of E_{esc} only normal modes exist. Up to about 55% of E_{esc} only regular modes exist, either normal or of higher-resonance type. At still higher energies irregular modes appear and are observed to dominate the phase space already at 90% of E_{esc}. Yet normal modes do not disappear and show a remarkable stability. The real possibility of monitoring such fine details, as e.g. the transition from regular to chaotic modes, is questionable and may be severely inhibited by solvent effects [7] that here have been neglected.

Secondly, comparing with other PSS calculations on two-degrees of freedom Hamiltonians, we observe that irregular modes are generated in the central portions of the PSS ensemble, and this behavior is consonant with that of the Hénon–Heiles Hamiltonian [10,18]. Instead, we think that α,α-trehalose will show a behavior which is more similar to the case of two coupled Morse oscillators, since the potential surface reported in the literature [13,14] resembles that of the two Morse oscillators [4,5,17].

Furthermore, in β,β-trehalose, chaotic mixing of torsions drives the system to rotations. Instead, for potentials similar to two coupled Morse oscillators, we expect to find modes (local modes) in which torsions decouple even at low energy. The phenomenon of local modes is *not* observed in β,β-trehalose.

The tensions f_Φ connected with the geometrical constraints are important [15]; they break the symmetry of the phase space with respect to the equilibrium angles, as is apparent at all energies in Fig. 2, and they cause the pure antisymmetric normal mode to be off the natural equilibrium. Indeed, stationary points

Fig. 3. The Poincaré Surface of Section in the plane (Φ' = phi', $p_{\Phi'} = p_{phi'}$) for various initial conditions at energy $E = 1500\ cm^{-1}$ (center of the figure) and Lissajous maps corresponding to the four fixed points (at the corners). Units for Φ' are degrees and for $p_{\Phi'}$ are $u^* = amu\ Å^{2\,\circ}/fs$.

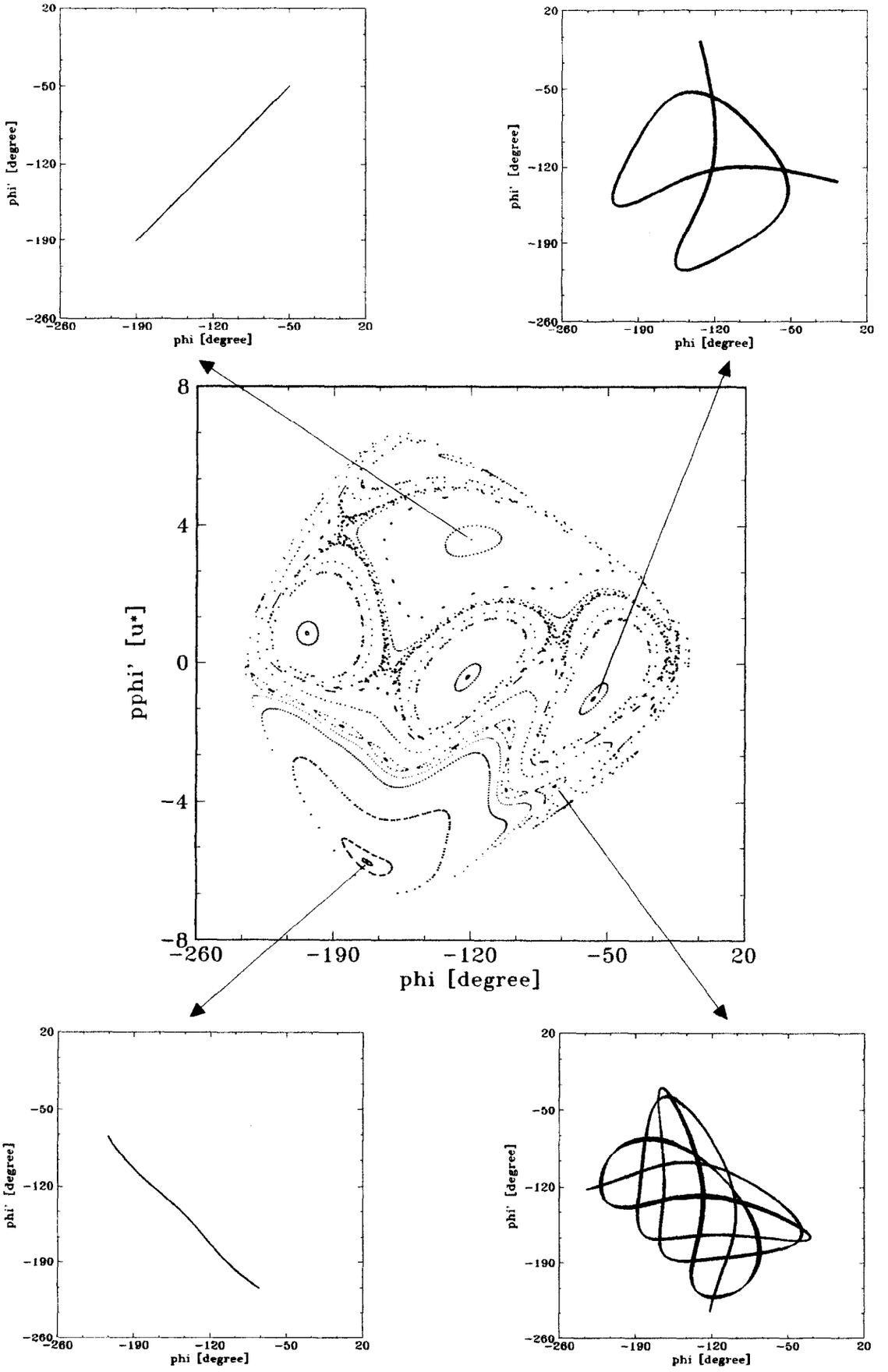
20
-50
-120
-190
-260
phi' [degree]
-260
-190
-120
-50
20
phi [degree]
8
4
0
-4
-8
pphi' [u*]

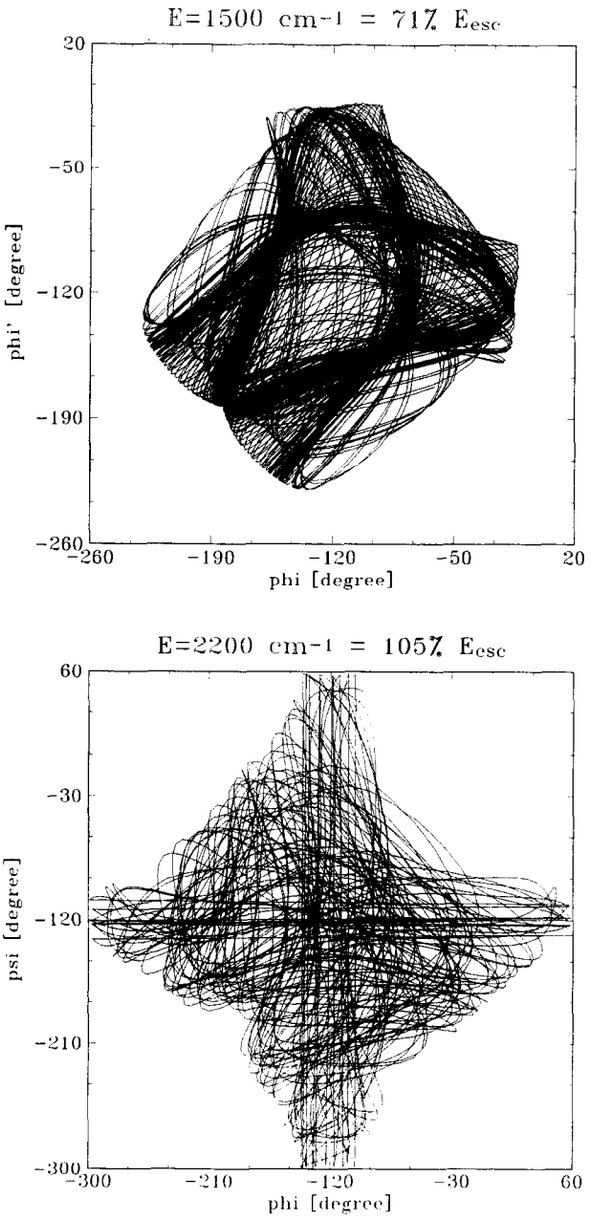

Fig. 4. The Lissajous maps of chaotic trajectories for two initial conditions at energies $E = 1500$ cm^{-1} (top) and $E = 2200$ cm^{-1} (bottom). Units for Φ,Φ' are degrees.

of the real potential V do not coincide with those of the potential associated with f_{Φ}. This effect is more pronounced at higher energies, and it should be kept in mind when imparting initial conditions in molecular dynamics programs.

A future development of the present work will be the integration of classical equations of motion with more realistic potentials. This implies that a potential defined numerically for discrete values of Φ and Φ' for each specific glycosidic linkage should be used instead of an analytically defined functional dependence of V on (Φ,Φ').

References

[1] M. Karplus and G.A. Petsko, *Nature*, 347 (1990) 631–638; P.A. Bash, U.C. Singh, R. Landridge, and P.A. Kollman, *Science*, 236 (1987) 564–568.
[2] H.E. Kandrup and M.E. Mahon, *Ann. New York Acad. Sci.*, 751 (1995) 93–111; C.V. Siopis, G. Contopouls, and H.E.. Kandrup, *Ann. New York Acad. Sci.*, 751 (1995) 205–212.
[3] D.W. Noid, M.L. Koszykowski, and R.A. Marcus, *J. Chem. Phys.*, 57 (1977) 404–408.
[4] C. Jaffé and P. Brumer, *J. Chem. Phys.*, 73 (1980) 5646.
[5] E.L. Sibert III, W.P. Reinhardt, and J.T. Hynes, *J. Chem. Phys.*, 77 (1982) 3583.
[6] J.W. Brady and R.K. Schmidt, *J. Phys. Chem.*, 97 (1993) 958–966; S.B. Engelsen, C. Hervé du Penhoat, and S. Pérez, *J. Phys. Chem.*, 99 (1995) 13334–13351.
[7] J.W. Brady, *J. Am. Chem. Soc.*, 108 (1986) 8153–8160; J.W. Brady, *J. Am. Chem. Soc.*, 111 (1989) 5155–5165.
[8] B.P. van Eijck, R.W.W. Hooft, and J. Kroon, *J. Phys. Chem.*, 97(1993) 12083–12089.
[9] M.C. Donnamaria, E.I. Howard, and J.R. Grigera, *J. Chem. Soc., Faraday Trans.*, 90 (1994) 2731–2735.
[10] A.J. Lichtenberg and M.A. Lieberman, *Regular and Chaotic Dynamics*, 2nd ed., Springer-Verlag, New York, 1992.
[11] E.B. Wilson Jr., J.C. Decius, and P.C. Cross, *Molecular Vibrations*, McGraw-Hill, New York, 1955.
[12] J.C. Decius, *J. Chem. Phys.*, 16 (1948) 1025–1034.
[13] I. Tvaroska, and L Vaklavik, *Carbohydr. Res.*, 60 (1987) 137–149.
[14] M.K. Dowd, P. Reilly, and A.D. French, *J. Comput. Chem.*, 13 (1992) 102–114.
[15] H. Goldstein, *Classical Mechanics*, Addison-Wesley, Reading, MA, 1951.
[16] *SSP Scientific and Statistical Package*, IBM Company.
[17] G. Longhi, S. Abbate, C. Zagano, G. Botto, and L. Ricard-Lespade, *Theor. Chim. Acta*, 82 (1992) 321–337.
[18] M. Hénon and C. Heiles, *Astron. J.*, 69 (1964) 73.